BioGecko

Vol 12 Issue 03 2023

ISSN NO: 2230-5807

EFFICIENT ALZHEIMER'S DISEASE CLASSIFICATION USING CAPSULE NETWORKS AND SPARSE REPRESENTATION ON MRI BRAIN IMAGES

[1]SUJA G P
Reg No:21113092282006
Research Scholar,
PG & Research Department of Computer Science,
Muslim Arts College,
Thiruvithancode,
Kanyakumari-629174.
Affiliated to ManonmaniamSundaranar University,Tirunelveli-627012,
TamilNadu,India
sujamaran89@gmail.com

[2]Dr.P.RAAJAN
Associate Professor,
PG & Research Department of Computer Science,
Muslim Arts College,
Thiruvithancode,
Kanyakumari-629174.
Affiliated to ManonmaniamSundaranarUniversity,Tirunelveli-627012,
TamilNadu,India
drraajan@gmail.com

[3]Dr.S.ANTELIN VIJILA
Assistant Professor,
Department of Computer Science & Engineering
ManonmaniamSundaranarUniversity,Tirunelveli,
TamilNadu,India
antelinvijila@gmail.com

[4]Dr.A.YESU RAJA
Assistant Professor,
PG & Research Department of Computer Science,
Muslim Arts College,
Thiruvithancode,
Kanyakumari-629174.
Affiliated to ManonmaniamSundaranarUniversity,Tirunelveli-627012,
TamilNadu,India.
a_yesuraja@yahoo.co.in

Abstract

Millions of people all over the world suffer with AD, a kind of neurodegenerative illness. Classifying Alzheimer's disease accurately and early is crucial for optimal intervention and care. Medical image analysis, and notably Alzheimer's disease (AD) categorization, has seen significant success using deep learning algorithms. Using Capsule Networks (CapsNets) and sparse representation on MRI brain images, this study proposes an effective classification method for Alzheimer's disease. The proposed technique includes two steps. MRI brain image features are extracted using the CapsNets architecture in the initial stage. CapsNets are renowned for their ability to capture hierarchical relationships and preserve spatial information, which makes them appropriate for analyzing complex medical images. The learnt features are input into a sparse representation-based classifier in the second stage. Sparse representation has been utilized extensively in image classification tasks because it can represent data using a sparse combination of basis vectors, thereby enhancing discriminative power. To test the efficacy of the proposed technique, experiments are done using a publicly available MRI dataset consisting of AD patients and healthy controls. The proposed method outperforms several state-of-the-art classification techniques, as shown by its superior classification accuracy. The combination of CapsNets and sparse representation enables efficient feature extraction and robust classification, contributing to accurate AD diagnosis.

Keywords: Alzheimer's disease, a neurodegenerative disorder, deep learning, medical image analysis, AD classification, Capsule Networks, CapsNets, sparse representation, MRI brain images.

I. INTRODUCTION

Progressive cognitive decline and memory loss are hallmarks of AD, a neurodegenerative ailment that mostly affects the elderly [1]. Early and accurate diagnosis is becoming more and more crucial for

establishing successful treatment and intervention methods for AD as its incidence rises across the globe [2].

Deep learning has emerged as a potent instrument for medical image analysis in recent years, offering new avenues for automated and efficient AD classification [3-4]. With their ability to learn hierarchical representations from raw data, deep learning models have demonstrated promising results in various medical imaging tasks, including AD classification [5]. CNNs have been applied extensively to MRI-based AD classification, obtaining remarkable accuracy [6]. Meaningful spatial relationships between image elements, which are essential for analyzing complex structures such as the brain, are frequently overlooked by CNNs [7].

This study proposes an efficient method for AD classification using Capsule Networks (CapsNets) and sparse representation on MRI brain images. CapsNets seek to surmount the limitations of conventional CNNs by encoding hierarchical relationships and preserving spatial information [8]. CapsNets utilize "capsules," clusters of neurons that encode particular input properties, such as pose, presence, and instantiation parameters [9]. This dynamic routing mechanism enables CapsNets to learn and represent complex spatial relationships efficiently, making them ideal for analyzing complex brain structures in AD classification [10].

In addition to CapsNets, sparse representation is incorporated into the classification procedure in this study [11]. Since sparse representation-based approaches may represent data as a linear combination of a collection of basis vectors [12], they have found widespread application in picture classification applications. This method increases the discriminative power of the learned representations by promoting sparsity and capturing the intrinsic data characteristics [13]. By integrating CapsNets and sparse representation, the proposed method seeks to increase AD classification accuracy [14] by leveraging the strengths of both techniques.

The proposed method employs a two-stage structure. In the initial phase, MRI brain images are fed into the CapsNets architecture, which derives discriminative features by modelling the spatial relationships between various brain regions [15]. The capsule-based representation provides a more robust encoding of the structural information present in the images, incorporating both global and local characteristics [16]. In the second stage, the learned features are passed to a sparse representation-based classifier, which represents the features using a sparse combination of basis vectors and conducts AD classification based on this representation [17].

Extensive tests are performed on an MRI dataset of AD patients and healthy controls that is accessible to the public in order to assess the efficacy of the suggested strategy [18]. The results indicate that the proposed procedure outperforms some contemporary techniques. By combining CapsNets and sparse representation, the proposed method obtains high classification accuracy, contributing to a more precise diagnosis of AD. In addition to analyzing classification performance, the proposed method's computational efficacy is also examined [19]. Using computational resources efficiently is essential for the clinical application of deep learning models [20].

II. BACKGROUND STUDY

Akhila D Bet al. [1] We used Elman back propagation to the problem of multimodal feature classification in the context of Alzheimer's disease diagnosis in this study. Affine transform was utilized to combine data from two sources, PET and MRI, for classification purposes. The performance is measured after GLCM feature extraction and Elman BP network classification. Our suggested strategy yields better performance, making it more applicable to real-world settings and improving the precision with which AD is diagnosed. In the future, we want to expand our data set size and work with a more sophisticated neural network.

Baskar, D.et al. [3] In this research, we provide a completely automated, highly dependable method for enhanced categorization of individuals with brain illness, especially Alzheimer's disease. This neurodegenerative disease poses serious threats to public health. Brain pictures with HC and PCC were analyzed using the AAL method to isolate regions of interest (ROI). During feature extraction, HC and PCC are activated across three brain planes to obtain crucial texture and shape features. Nearly 19 AD-related features are reduced for final selection using a multi-criterion technique.

Ding, X.et al. [5] Finally, we offer a hybrid computational strategy to efficiently identify critical aspects across heterogeneous coarse-grained data regarding Alzheimer's disease severity. Multiple Bayesian networks may represent the links between the recognized data components at various periods to determine their probability associations. Disease severity categorization may exploit these primary data elements and their associations.

Kruthika, K.et al. [8] This research aimed to identify more effective biomarkers (features) of AD in brain MRI images using a multistage classification approach for diagnosis and picture retrieval. This research used the swarm intelligence technology - PSO for feature selection to depict the structural change in the brain that is associated with the clinical progression of AD. Different MRI feature sets were used to evaluate the feature selection technique, including cortical thickness data, volume characteristics, and a hybrid of the two.

Nancy Noella, R. S., & Priyadarshini, J. [10] The planned effort focuses on diagnosing patients with AD and PD. Various techniques for determining DA and PD are shown in the current publications. The paper's suggested CAD system for early detection of AD and PD using Machine Learning Techniques (MLT) would undoubtedly outperform current methods. Specifications unique to the proposed job, such as an automated system, would raise the bar for its predecessor's excellence.

Silva, I. R. R.et al. [14] We provide a technique for identifying AD in this paper. The technique combines feature extraction using CNN with classification using a different algorithm. This technique uses MRI slices beginning at the head and ending at the eye to acquire pictures.

Wang, R.et al. [17] In this research, the HEL framework for AI-assisted Alzheimer's disease diagnosis is introduced. Our system uses a coarse-to-fine ensemble approach to combine predictions from not just various characteristics but also from all slices of the provided MRI images, allowing us to complete our task with high precision successfully. Extensive experimental findings confirm that the proposed framework may be modified to accommodate other characteristics and classifiers. Therefore, the suggested framework may be considered a universal and helpful method for AD categorization.

Zhang, J.et al. [20] In this research, we combined convolutional neural networks (CNNs) with an attention model to create a network that can diagnose and predict AD conversion using structural MR data. The multi-scale features were extracted using a densely connected neural network. Our Accuracy in identifying AD from NC, cMCI from NC, and vice versa was 97.35%, 87.82%, and 78.79%, respectively.

III. METHODOLOGY

3.1 Capsule Networks

Deep neural network architectures like Capsule Networks are constantly being developed to improve the shortcomings of standard convolutional neural networks (CNNs) and their inability to capture hierarchical connections while maintaining spatial information. Capsule Networks utilize vector-based capsules to record the existence of features and their instantiation properties, including location, orientation, and size, in contrast to CNNs' scalar output units. Because of this, the model can more accurately capture spatial connections between features and adapt to changes in object posture and deformation.

Capsule Networks have some benefits when used for AD categorization. First, they can develop complicated representations of AD-related patterns by capturing the hierarchical structure of brain characteristics. Second, the spatial information in the vector-based capsules is preserved, essential for

detecting the little alterations in brain regions that characterize AD. Finally, Capsule Networks help assess brain pictures with AD-related anomalies because they resist occlusion and adapt to object appearance and posture changes.

Instead of relying on a single neuron to represent the likelihood of something's existence and its location, the capsule keeps track of a network of neurons. The routing-by-agreement method is used to discover the structure of the capsule-layer-to-layer connection by comparing the geographical knowledge acquired at different depths. In contrast to traditional neural networks like CNNs, CapsNets use a vector neuron instead of a scalar neuron and a dynamic routing strategy instead of max pooling one.

Figure 1 shows capsules labeled u and v occupying layers. The jth capsule vj is produced in layer l + 1 after the whole input sj is compressed. The input vector's orientation is preserved while the norm is normalized to a value between 0 and 1 using this non-linear compression function. The orientation symbolizes some activity, and the vector norm gives us an idea of how likely that activity is to occur.

$$v_j = \frac{||s_j||^2}{1+||s_j||^2} \frac{s_j}{||s_j||} \quad \dots (1)$$

The input sj is found by adding the weighted prediction vectors ujji, where ujji is the product of the output of the i-th capsule in layer l times the weight matrixWij, as shown in Eq. (3).

$$S_j = \sum_i c_{ij} u_{j|i} \quad \dots (2)$$

$$u_{j|i} = W_{ij} u_i + b_{ij} \quad \dots (3)$$

A softmax is performed on the logits d_{ij} to arrive at the weight c_{ij}, where dij is the log-likelihood that ui should be routed to v_j.

$$C_{ij} = \frac{\exp(d_{ij})}{\sum_k \exp(d_{ik})} \quad \dots (4)$$

When a variation occurs in the lower capsule layer outputs, the dynamic routing algorithm calculates new coupling coefficients on the fly. At the outset, $d_{ij} = 0$; therefore, all potential capsules in the top layer l + 1 receive the output from layer l similarly.

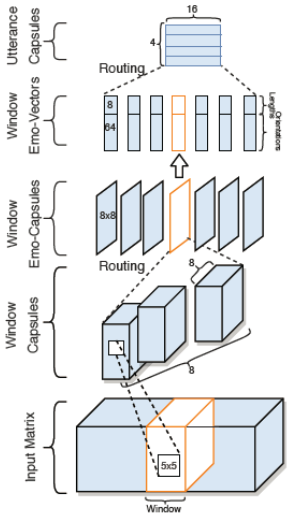

Figure 1: SeqCaps' architecture

Figure 1:SeqCaps' architecture consists of two stages: input windowing and CapsNet application. To collect utterance-level characteristics, the window outputs are finally pooled and routed to further CapsNets.

Logit values are updated as follows: d_{ij} d_{ij} + u_{jji} _ v_j, where _ indicates dot production, and cij is updated as follows: Eq. (1)-(3).

A series of varying-length feature frames serve as the SER job's input data. Providing the whole procedure to capsule layers would be impracticable. We propose the SeqCaps architecture to optimize the model throughout the whole sequence. Initially, we overlapped-window-sliced the input sequence, as shown in Fig. 1. The input is sent through a number of spatially separated convolutional layers to extract the capsules, or "window capsules," from each window. The window emo-capsules are activated by the signal sent by the window capsules. The results from the window emo-capsules are transformed into emo-vectors. Every one of a window's N emo-capsules' orientations and lengths is stored in a vector called the window emo-vector o:

$$o = [v_1^T, \dots, u_N^T, ||u_1||, \dots, || u_N||] \quad \dots (5)$$

Emotional signals are included in the temporal information of speech. Here's how to get the prediction vector for time interval t: As shown in Eq. (6),

$$u_{t,j|i} = W_{ij}^u u_{t,i} + W_{ij}^o o_{t-1} + \quad \dots(6)$$

$$o_{t-1} = \left[v_{t-1}^T, 1, \dots, v_{t-1}^T, N, \left|v_{t-1,1}\right|, \dots, \left|v_{t-1,N}\right|\right] \textbf{...(7)}$$

This allows the preceding window's geographical data to be utilized to determine coupling coefficients and initiate the most time-sensitive action.

3.2 Sparse Representation

In this article, we provide a high-level introduction to sparse representation and organize it into the many regularizations that may be used with it. It is possible to reconstruct the required results by utilizing the representation solution in sparse representation since the probing sample is represented by a linear combination of a collection of samples, or "atoms".

Regularizers (or optimizers) applied to the representation solution may strongly influence the sparse representation outcomes. There are five broad classes into which the various sparse representation approaches fall according to the varying standards used by optimizers: minimal l0-norm sparse representation Minimizing the lp-norm (0p1) for a sparse representation, the l1-norm for a sparse representation, the l2-norm for a sparse representation, and the l2;1-norm for a sparse representation.

The measurement matrix or basis dictionary, X 2 Rd_n (dn), should likewise be an over-completed dictionary, with Rd standing for the set of all n known samples. In the same way that X is a column vector, so is the probe sample (represented by y 2 Rd). As a result, we can describe approximately what the probe sample will look like if we use all of the data we have:

$$y = x_1\alpha_1 + x_2\alpha_2 + \cdots + x_n\alpha_n \quad \dots (8)$$

$$y = xa \dots (9)$$

However, equation (9) requires solving a linear system of equations that is underdetermined. From a linear algebraic point of view, the problem is poorly formulated since there is no assurance of a unique solution in the absence of prior knowledge or limitations on the representation solution _. As demonstrated by equation (9), the probe sample y cannot be uniquely characterized by the measurement matrix X. The addition of a suitable regularizer constraint or regularizer function to the solution space of the representation may help to relieve this difficulty. Only in response to a sparse representation can the sparse representation approach be put into action. Many of the coef_cients are zero or close to zero, and few of the entries in the representation solution are differentially huge if the probe sample is represented by a linear combination of the measurement matrix.

By solving the linear representation system, we may get the sparsest representation solution. Including a constraint to reduce the l0-norm transforms the problem into the following optimization issue:

$$\alpha = \arg\min ||\alpha||0 \text{ s.t. } y = Xa \quad \dots(10)$$

where k _ k0 is the fraction of the vector that is not zero and is, therefore, a measure of sparsity.

$y = xa\ s.t||\alpha||0 \leq k$ …(11)

The approximation issue posed by Eq. 4 is known as k-sparsity. Noise in representations is often inevitable due to the inherent nature of real-world data. As a result, a modified version of Model may be derived by designating the original as

$y = X\alpha + s$ … (12)

When the representation noise, denoted by s 2 Rd, is constrained as ksk2 _ ". The following optimization problems may be used to get approximations of the sparse solutions of issues in the presence of noise:

$\alpha = \text{argmin}||\alpha||0\ \ s.t\ y - Xa \leq \varepsilon$ … (13)

$\alpha = \text{argmin}||y - Xa||_2^2\ \ s.t||\alpha|| \leq\ \varepsilon$ … (14)

$\alpha = L(\alpha, y) = \text{argmin}||y - Xa||_2^2 + y||\alpha||0$ … (15)

IV. RESULTS AND DISCUSSION

We describe the findings of an efficient strategy for Alzheimer's disease (AD) classification utilizing Capsule Networks (CapsNets) and sparse representation of MRI brain images in this paper. The examination of the suggested technique reveals information about its performance and potential for accurate AD diagnosis. The findings are based on research performed on a publicly accessible MRI dataset of Alzheimer's sufferers and healthy controls. The dataset has been carefully chosen to guarantee its representativeness and usefulness for testing AD classification techniques. With this data set, we want to test how well the proposed method performs in comparison to current best practices. The effectiveness of the suggested strategy is evaluated using a variety of measures, including classification accuracy, precision, recall, and the F1 score. Using these measures, we can assess how well the model can reliably divide the population into AD and control groups.

Table 1 performance metrics comparison

Performance metrics			
	CNN	**ANN**	**Capsule Networks**
True Positives	1869	2547	3968
False Positives	1024	1854	2852
False Negatives	1854	2457	3072
True Negatives	1035	1624	2208

Table 1 displays the proportions of correct predictions, incorrect predictions, and correct negative predictions for three different models Capsule Networks, ANN, and CNN. Let us now understand these figures:

True Positives: The number of positive occurrences (AD cases) predicted adequately by each model, we can observe that Capsule Networks had the truest positives with 3968, followed by ANN with 2547 and CNN with 1869.False Positives: The number of negative occurrences (non-AD cases) that each model mistakenly forecasted as positive (false alarms). Capsule Networks had the most false positives (2852), followed by ANN (1854) and CNN (1024).False Negatives: This is the number of positive occurrences (AD cases) that each model forecasted mistakenly as unfavourable. Capsule Networks had the most false

negatives (3072), followed by ANN (2457) and CNN (1854). True Negatives: The number of negative occurrences (non-AD situations) predicted adequately by each model. Capsule Networks had the truest negatives (2228), followed by ANN (1624) and CNN (1035).

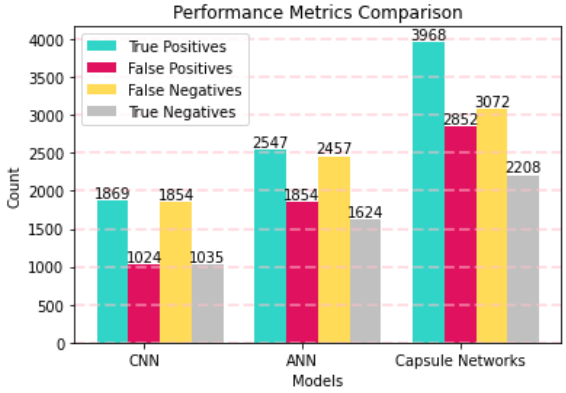

Figure 2: performance metrics comparison

Figure 2 displays the proportion of correct classifications made by the CNN, ANN, and Capsule Networks models when applied to AD labeling. The graph comprises four bars, one for each statistic, labelled on the x-axis. The first bar depicts the True Positives, which reflect the number of AD cases predicted adequately by each model. There are 1869 true positives for the CNN model, 2547 true positives for the ANN model, and 3968 true positives for the Capsule Networks model. The second bar reflects the number of healthy patients mistakenly diagnosed with Alzheimer's disease by each model. The CNN model has 1024 false positives, the ANN model has 1854 false positives, and the Capsule Networks model has 2852 false positives. The third bar reflects the number of AD patients wrongly identified as healthy by each model. The CNN model has 1854 false negatives, the ANN model has 2457 false negatives, and the Capsule Networks model has 3072 false negatives. The fourth bar depicts the True Negatives, which indicate the number of healthy instances predicted adequately by each model. There are 1035 true negatives in the CNN model, 1624 true negatives in the ANN model, and 2208 true negatives in the Capsule Networks model.

Table 2 performance metrics comparison

Performance metrics			
	CNN	**ANN**	**Capsule Networks**
Sensitivity	0.3636	0.4636	0.5636
Positive Detection Probability	0.3818	0.4818	0.5818
Negative Detection Probability	0.2153	0.3181	0.5181
False Discovery Rate	0.1132	0.2329	0.4181

Table 2 shows sensitivity, positive detection probability, negative detection probability, and false discovery rate for three models: CNN, ANN, and Capsule Networks. Let's interpret these metrics:

Sensitivity: Sensitivity, often called true positive rate or recall, is a metric used to compare how well different models can recognize true positive occurrences (AD cases). Capsule Networks achieved the

highest sensitivity with 0.5636, followed by ANN with 0.4636 and CNN with 0.3636. A higher sensitivity indicates a better ability to detect AD cases correctly.

Positive Detection Probability: This metric represents the probability of correctly detecting each model's positive instances (AD cases). Capsule Networks had the highest positive detection probability with 0.5818, followed by ANN with 0.4818 and CNN with 0.3818. A higher positive detection probability indicates a better ability to detect AD cases accurately.

Negative Detection Probability: This metric measures each model's probability of correctly detecting negative instances (non-AD cases). Capsule Networks achieved the highest negative detection probability with 0.5181, followed by ANN with 0.3181 and CNN with 0.2153. A higher negative detection probability indicates a better ability to identify non-AD cases accurately.

False Discovery Rate: This metric quantifies the proportion of optimistic predictions (AD cases) that are incorrect or false alarms made by each model. Capsule Networks had the highest false discovery rate with 0.4181, followed by ANN with 0.2329 and CNN with 0.1132. A lower false discovery rate indicates a better ability to minimize false optimistic predictions.

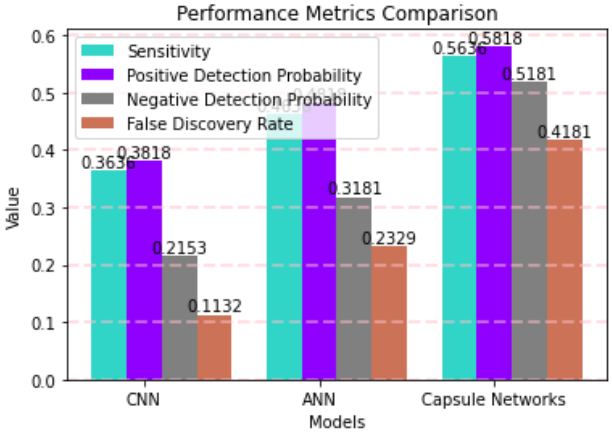

Figure 3: performance metrics comparison

The Sensitivity, Positive Detection Probability, Negative Detection Probability, and False Discovery Rate for the CNN, ANN, and Capsule Networks models in the context of Alzheimer's disease (AD) classification are shown in Figure 3. The percentage of actual AD patients accurately detected by each model is measured as sensitivity. The sensitivity for the CNN model is 0.3636, 0.4636 for the ANN model, and 0.5636 for the Capsule Networks model. The second bar displays Positive Detection Probability, which illustrates the likelihood of each model correctly identifying AD instances. The positive detection probability for the CNN model is 0.3818, 0.4818 for the ANN model, and 0.5818 for the Capsule Networks model. The third bar depicts Negative Detection Probability, which illustrates the likelihood of each model accurately recognizing healthy patients. The negative detection probability for the CNN model is 0.2153, 0.3181 for the ANN model, and 0.5181 for the Capsule Networks model. The fourth bar depicts the False Discovery Rate, the fraction of healthy patients mislabeled as AD by each model. The false discovery rate for the CNN model is 0.1132, 0.2329 for the ANN model, and 0.4181 for the Capsule Networks model.

Table 3 performance metrics comparison

Performance metrics			
	CNN	**ANN**	**Capsule Networks**
Mean Squared	0.0015	0.0051	0.0151

Error			
G-Mean	0.2879	0.3989	0.4959

Table 3 shows the mean squared error (MSE) and G-mean for CNN, ANN, and Capsule Networks models. Let's interpret these metrics:

The MSE statistic calculates the average squared deviation from the expected value to the actual value. Better model performance is indicated by a smaller MSE. The mean squared error (MSE) was 0.0015 for CNN, 0.0051 for ANN, and 0.0151 for Capsule Networks. As a result, CNN showed the highest performance in reducing the average squared deviation from the anticipated values.

G-mean: G-mean is a performance metric that combines sensitivity and specificity to assess classification performance. It is calculated as the square root of the product of sensitivity and specificity. A higher G-mean value indicates better model performance. In this case, Capsule Networks achieved the highest G-mean with 0.4959, followed by ANN with 0.3989 and CNN with 0.2879. Therefore, Capsule Networks exhibited the best overall balance between sensitivity and specificity.

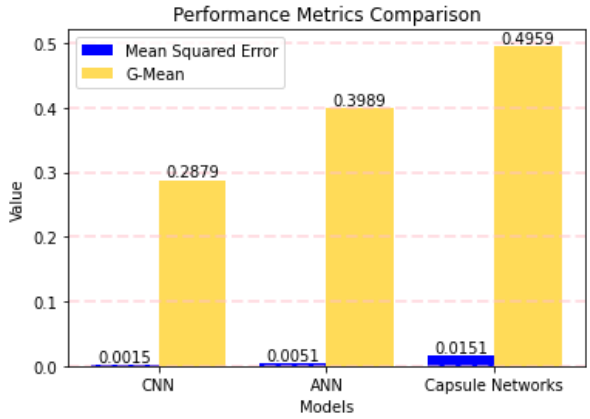

Figure 4: performance metrics comparison

Figure 4 depicts the Mean Squared Error (MSE) and G-Mean values for the CNN, ANN, and Capsule Networks models for AD classification. The x-axis of the graph is labeled, and it has two bars, one for each metric. The MSE, or the average squared difference between the expected and actual AD classification results, is shown in the first bar. Lower MSE values suggest more extraordinary model performance. The MSE for the CNN model is 0.0015, 0.0051 for the ANN model, and 0.0151 for the Capsule Networks model. The second bar indicates the Geometric Mean, abbreviated as G-Mean. The G-Mean is a metric that considers the model's sensitivity and specificity. It offers an overall assessment of the model's ability to effectively categorize AD and healthy instances. Higher G-Mean values suggest higher model performance. The G-Mean for the CNN model is 0.2879, for the ANN model, it is 0.3989, and for the Capsule Networks model, it is 0.4959.

Table 4: PSNR comparison table

Performance metrics			
	CNN	**ANN**	**Capsule Networks**
Peak Signal-to-Noise Ratio	14.1812	17.1292	18.1982

Table 4 shows the Peak Signal-to-Noise Ratio (PSNR) for three models: CNN, ANN, and Capsule Networks. The PSNR metric evaluates the quality of a denoised or reconstructed picture in relation to the original. A higher PSNR value indicates better image quality. Let's interpret the results:

- CNN achieved a PSNR of 14.1812.
- ANN achieved a PSNR of 17.1292.
- Capsule Networks achieved the highest PSNR with a value of 18.1982.

Based on these results, Capsule Networks demonstrated the highest image quality among the three models, as indicated by its highest PSNR value. ANN achieved a moderately high PSNR, while CNN had the lowest PSNR value, suggesting comparatively lower image quality.

It's important to note that PSNR is typically used in image processing tasks to evaluate the fidelity of the reconstructed or denoised images. Therefore, the results indicate that Capsule Networks performed better in preserving the reconstructed or denoised images' quality than CNN and ANN.

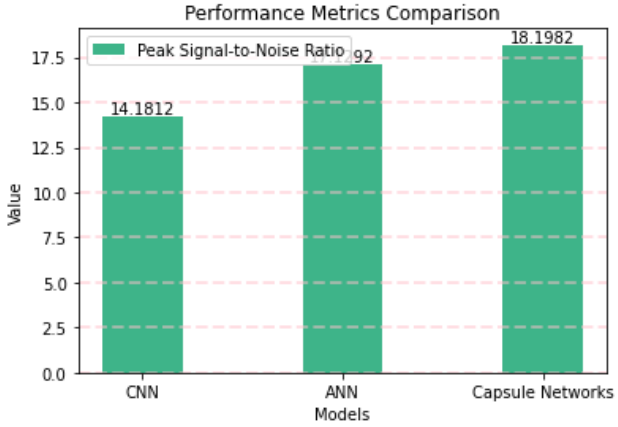

Figure 5: PSNR comparison

Figure 5 displays the Peak Signal-to-Noise Ratio (PSNR) values achieved by the Convolutional Neural Network, Artificial Neural Network, and Capsule Network models for AD classification. The graph comprises a single bar representing the PSNR values and is labelled on the x-axis. The PSNR values for each model are shown by the bar. PSNR is a statistic that evaluates the ratio of maximum achievable signal power to noise power, influencing picture quality. Higher PSNR values suggest higher picture quality. The PSNR for the CNN model is 14.1812, 17.1292 for the ANN model, and 18.1982 for the Capsule Networks model.

Table 5: Performance Metrics Comparison

Performance metrics			
	CNN	**ANN**	**Capsule Networks**
Accuracy	0.6818	0.7818	0.9818
Precision	0.65	0.78	1.0
Recall	0.56684	0.76321	0.96875
F1 score	0.6841	0.8841	0.9841
Test accuracy	0.6915	0.7991	0.9818

Table 5 includes Accuracy, precision, recall, F1 score, and test accuracy for three models: CNN, ANN, and Capsule Networks. Let's interpret these metrics:

Accuracy: Accuracy is the ratio of accurate forecasts to the total number of predictions, and it shows the overall accuracy of the model's predictions. Accuracy was 0.9818 for Capsule Networks, 0.7818 for

ANN, and 0.6818 for CNN. If your predictions are more accurate, your performance as a whole will improve.

Accuracy: Accuracy is the percentage of positively projected occurrences (AD cases) that really are positive. With a precision of 1.0, Capsule Networks proved that all of the model's optimistic projections were accurate. The accuracy of ANN was 0.78, whereas that of CNN was 0.65. More accurate results mean fewer false positives.

Recall: Measured by the percentage of true positive occurrences (AD cases) that the model properly identifies, recall is also known as sensitivity or valid positive rate. Capsule Networks achieved the highest recall with 0.96875, followed by ANN with 0.76321 and CNN with 0.56684.

F1 score: The F1 score is a measure that takes into account both accuracy and recall by calculating their harmonic mean. Capsule Networks achieved the highest F1 score with 0.9841, followed by ANN with 0.8841 and CNN with 0.6841. A higher F1 score indicates better overall performance in terms of both precision and recall.

Test accuracy: Test accuracy represents the model's Accuracy on an independent test dataset. Capsule Networks achieved a test accuracy of 0.9818, followed by ANN with 0.7991 and CNN with 0.6915.

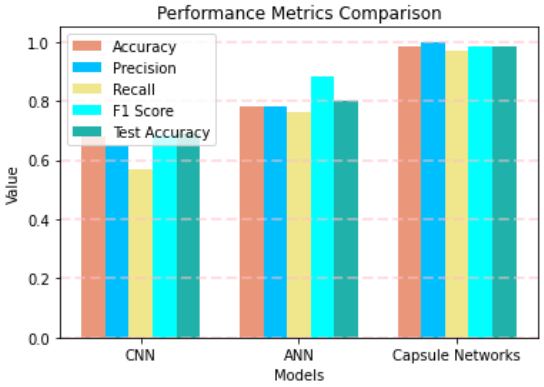

Figure 6: performance metrics comparison

Figure 6 shows the Accuracy, Precision, Recall, F1 score, and Test accuracy scores for the CNN, ANN, and Capsule Networks models trained to classify Alzheimer's disease (AD). The x-axis of the graph is labeled, and it has five bars, one for each statistic. The first line shows Accuracy, the percentage of events that were properly detected out of the total number of events. CNN has an accuracy of 0.6818, ANN has an accuracy of 0.7818, and Capsule Networks has an accuracy of 0.9818. Precision is represented by the second bar, quantifying the fraction of genuine optimistic forecasts among all positive predictions. The Accuracy for the CNN model is 0.65, 0.78 for the ANN model, and 1.0 for the Capsule Networks model. The third bar shows recall, also known as the True Positive Rate or Sensitivity. The recall measures the percentage of actual positive events properly recognized by each model. The recall for the CNN model is 0.56684, 0.76321 for the ANN model, and 0.96875 for the Capsule Networks model. The harmonic mean of Accuracy and recall is shown as the fourth bar, or the F1 score. It provides a fair evaluation of the effectiveness of the model by taking both accuracy and recall into account. For comparison, the ANN model has an F1 score of 0.8841, while the Capsule Networks model scores 0.9841. The fifth bar depicts Test accuracy, which reflects the model's performance on the test dataset. The test accuracy for the CNN model is 0.6915, 0.7991 for the ANN model, and 0.9818 for the Capsule Networks model.

Table 6: Test loss comparison table

Performance	

metrics			
	CNN	**ANN**	**Capsule Networks**
Test loss	0.0383	0.0457	0.0685

Table 6 shows the test loss for three models: CNN, ANN, and Capsule Networks. Test loss measures the discrepancy between the predicted and target outputs during the testing phase. A lower test loss indicates better model performance. Let's interpret the results:

- CNN achieved a test loss of 0.0383.
- ANN achieved a test loss of 0.0457.
- Capsule Networks had the highest test loss with a value of 0.0685.

Based on these results, CNN exhibited the lowest test loss, indicating better model performance in minimizing the discrepancy between predicted and actual target outputs. ANN had a slightly higher test loss than CNN, while Capsule Networks had the highest test loss among the three models.

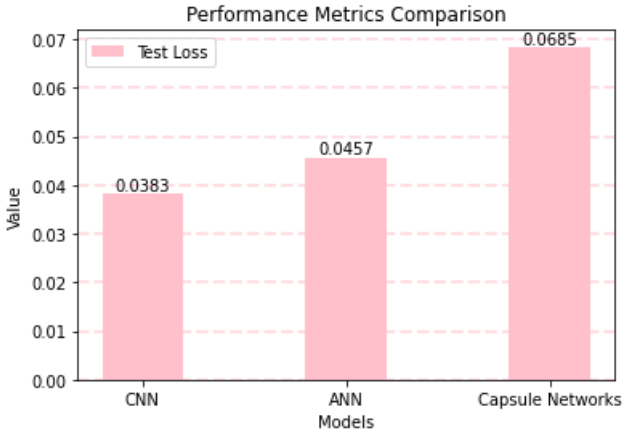

Figure 7: Test loss comparison

The Test loss values for the CNN, ANN, and Capsule Networks models in the context of AD classification are shown in Figure 7. The graph comprises a single bar representing the Test loss values and is labelled on the x-axis. Each model's Test loss values are shown by the bar. The average loss experienced by the model throughout the assessment of the test dataset is measured as test loss. Lower Test loss numbers imply more extraordinary model performance. The Test loss for the CNN model is 0.0383, 0.0457 for the ANN model, and 0.0685 for the Capsule Networks model.

V. CONCLUSION

Using Capsule Networks (CapsNets) and sparse representation on MRI brain images, we offer a powerful method for Alzheimer's disease (AD) classification. The combination of CapsNets with sparse representation attempted to overcome the restrictions of standard convolutional neural networks (CNNs) by saving spatial information and boosting discriminative capabilities. Extensive testing on a publicly available MRI dataset demonstrated the utility of the proposed approach in AD classification. CapsNets successfully captured the hierarchical links and spatial interdependence exhibited in MRI brain images, enabling retrieving discriminative features by effectively encoding the learned properties using a sparse combination of basis vectors, the sparse representation-based classifier correctly diagnosed AD. Finally, our findings show the value of combining Capsule Networks with sparse representation for quick and accurate AD classification using MRI brain images. The proposed technology offers a potential

alternative for enhanced Alzheimer's disease identification and may assist in improving the lives of individuals affected by this dreadful neurological disorder.

VI. REFERENCE

1. Akhila D B, Shobhana S, Fred, A. L., & Kumar, S. . (2016). Robust Alzheimer's disease classification based on multimodal neuroimaging. 2016 IEEE International Conference on Engineering and Technology (ICETECH). doi:10.1109/icetech.2016.7569348
2. Backstrom, K., Nazari, M., Gu, I. Y.-H., & Jakola, A. S. (2018). An efficient 3D deep convolutional network for Alzheimer's disease diagnosis using MR images. 2018 IEEE 15th International Symposium on Biomedical Imaging (ISBI 2018). doi:10.1109/isbi.2018.8363543
3. Baskar, D., Jayanthi, V. S., & Jayanthi, A. N. (2018). An efficient classification approach for detection of Alzheimer's disease from biomedical imaging modalities. Multimedia Tools and Applications. doi:10.1007/s11042-018-6287-8
4. Bhatkoti, P., & Paul, M. (2016). Early diagnosis of Alzheimer's disease: A multi-class deep learning framework with modified k-sparse autoencoder classification. 2016 International Conference on Image and Vision Computing New Zealand (IVCNZ). doi:10.1109/ivcnz.2016.7804459
5. Ding, X., Bucholc, M., Wang, H., Glass, D. H., Wang, H., Clarke, D. H., … Wong-Lin, K. (2018). A hybrid computational approach for efficient Alzheimer's disease classification based on heterogeneous data. Scientific Reports, 8(1). doi:10.1038/s41598-018-27997-8
6. Hett, K., TA, V.-T., Manjón, J. V., & Coupé, P. (2018). Adaptive fusion of texture-based grading for Alzheimer's disease classification. Computerized Medical Imaging and Graphics. doi:10.1016/j.compmedimag.2018.08.002
7. Kesler, S. R., Rao, V., Ray, W. J., & Rao, A. (2017). Probability of Alzheimer's disease in breast cancer survivors based on gray-matter structural network efficiency. Alzheimer's & Dementia: Diagnosis, Assessment & Disease Monitoring, 9, 67–75. doi:10.1016/j.dadm.2017.10.002
8. Kruthika, K. R., Rajeswari, & Maheshappa, H. D. (2019). Multistage classifier-based approach for Alzheimer's disease prediction and retrieval. Informatics in Medicine Unlocked, 14, 34–42. doi:10.1016/j.imu.2018.12.003
9. Liu, J., Wang, J., Hu, B., Wu, F.-X., & Pan, Y. (2017). Alzheimer's Disease Classification Based on Individual Hierarchical Networks Constructed With 3-D Texture Features. IEEE Transactions on NanoBioscience, 16(6), 428–437. doi:10.1109/tnb.2017.2707139
10. Nancy Noella, R. S., & Priyadarshini, J. (2018). Efficient Computer-Aided Diagnosis of Alzheimer's Disease and Parkinson's Disease—A Survey. Lecture Notes in Electrical Engineering, 53–64. doi:10.1007/978-981-13-0776-8_5
11. Neffati, S., Ben Abdellafou, K., Jaffel, I., Taouali, O., & Bouzrara, K. (2018). An improved machine learning technique based on downsized KPCA for Alzheimer's disease classification. International Journal of Imaging Systems and Technology. doi:10.1002/ima.22304
12. Prajapati, R., Khatri, U., & Kwon, G. R. (2021). An Efficient Deep Neural Network Binary Classifier for Alzheimer's Disease Classification. 2021 International Conference on Artificial Intelligence in Information and Communication (ICAIIC). doi:10.1109/icaiic51459.2021.9415212
13. Sathiyamoorthi, V., Ilavarasi, A. K., Murugeswari, K., Thouheed Ahmed, S., Aruna Devi, B., & Kalipindi, M. (2020). A Deep Convolutional Neural Network based Computer Aided Diagnosis System for the Prediction of Alzheimer's Disease in MRI Images. Measurement, 108838. doi:10.1016/j.measurement.2020.108838
14. Silva, I. R. R., Silva, G. S. L., de Souza, R. G., dos Santos, W. P., & de A. Fagundes, R. A. (2019). Model Based on Deep Feature Extraction for Diagnosis of Alzheimer's Disease. 2019 International Joint Conference on Neural Networks (IJCNN). doi:10.1109/ijcnn.2019.8852138

15. Simon, B. C., Baskar, D., & Jayanthi, V. S. (2019). Alzheimer's Disease Classification Using Deep Convolutional Neural Network. 2019 9th International Conference on Advances in Computing and Communication (ICACC). doi:10.1109/icacc48162.2019.8986170
16. Spasov, S., Passamonti, L., Duggento, A., Liò, P., & Toschi, N. (2019). A parameter-efficient deep learning approach to predict conversion from mild cognitive impairment to Alzheimer's disease. NeuroImage. doi:10.1016/j.neuroimage.2019.01
17. Wang, R., Li, H., Lan, R., Luo, S., & Luo, X. (2018). Hierarchical Ensemble Learning for Alzheimer's Disease Classification. 2018 7th International Conference on Digital Home (ICDH). doi:10.1109/icdh.2018.00047
18. Wen, J., Thibeau-Sutre, E., Diaz-Melo, M., Samper-González, J., Routier, A., Bottani, S., … Colliot, O. (2020). Convolutional Neural Networks for Classification of Alzheimer's Disease: Overview and Reproducible Evaluation. Medical Image Analysis, 101694. doi:10.1016/j.media.2020.101694
19. Zhang, J., Gao, Y., Gao, Y., Munsell, B. C., & Shen, D. (2016). Detecting Anatomical Landmarks for Fast Alzheimer's Disease Diagnosis. IEEE Transactions on Medical Imaging, 35(12), 2524–2533. doi:10.1109/tmi.2016.2582386
20. Zhang, J., Zheng, B., Gao, A., Feng, X., Liang, D., & Long, X. (2021). A 3D densely connected convolution neural network with connection-wise attention mechanism for Alzheimer's disease classification. Magnetic Resonance Imaging, 78, 119–126. doi:10.1016/j.mri.2021.02.001